European Journal of Drug Metabolism and Pharmacokinetics

Supplementary Material

Title: Management of drug interactions with inducers: onset and disappearance of induction on cytochrome P450 3A4 and uridine diphosphate glucuronosyltransferase 1A1 substrates

Authors: Sara Bettonte [1, 2], Mattia Berton [1, 2], Felix Stader [3], Manuel Battegay [1, 2], and Catia Marzolini [1,2,4]

Affiliations: 1 Division of Infectious Diseases and Hospital Epidemiology, Departments of Medicine and Clinical Research, University Hospital Basel, 4031 Basel, Switzerland

2 Faculty of Medicine, University of Basel, 4031 Basel, Switzerland

3 Certara UK Limited, Sheffield, UK

4 Department of Molecular and Clinical Pharmacology, University of Liverpool, L69 3GF Liverpool, UK

Corresponding author:

Sara Bettonte

Division of Infectious Diseases and Hospital Epidemiology

Departments of Medicine and Clinical Research

University Hospital Basel

Petersgraben 4

4051 Basel, Switzerland

E-mail: sara.bettonte@unibas.ch

Alternative corresponding author:

Catia Marzolini

Division of Infectious Diseases and Hospital Epidemiology

Departments of Medicine and Clinical Research

University Hospital Basel

Petersgraben 4

4051 Basel, Switzerland

E-mail: catia.marzolini@usb.ch

Supplementary Table 1. Parameters of the simulated drugs.

Parameter	Unit	Dolutegravir		Raltegravir		Rifampicin		Efavirenz		Rifabutin	
Physicochemical properties											
molecular weight	g/mol	419	[1]	445.16	[2]	823	[3]	315.7	[4]	847.02	[5]
log P		2.2	[1]	0.58	[2]	3.28	[3]	4.6	[4]	3.2	[5]
drug type		ma	[6]	ma	[7]	zwitterion	[3]	ma	[8]	ma	[9]
pK_{a1}		8.3	[1]	6.67	[2]	1.7	[3]	10.2	[4]	6.9	[10]
pK_{a2}		-		-		7.9	[3]	-		-	
BP		0.55	[7]	0.6	[2]	0.9	[3]	0.74	[4]	0.6	[11]
fu_p		0.007	[7]	0.17	[2]	0.15	[3]	0.02	[4]	0.15	[12]
binding protein		albumin	[13, 14]	albumin	[15]	albumin	[16, 17]	albumin	[18]	albumin	[19]
Absorption											
P_{app}	10^{-6} cm/sec	0.868	[7]	1.6	[2]	1.472	retrograde calculation	2.5	[4]	9.5	[11]
Metabolism and Elimination											
CYP3A4 CL_{int}	µl/min/pmol enzyme	0.0035	retrograde calculation	-		0.0036	retrograde calculation	0.007	[4]	0.514	[11]
CYP3A5 CL_{int}	µl/min/pmol enzyme	-		-		-		0.03	[4]	-	
CYP2B6 CL_{int}	µl/min/pmol enzyme	-		-		-		0.55	[4]	-	
CYP2A6 CL_{int}	µl/min/pmol enzyme	-		-		-		0.08	[4]	-	
CYP1A2 CL_{int}	µl/min/pmol enzyme	-		-		-		0.07	[4]	-	
UGT1A1 CL_{int}	µl/min/pmol enzyme	0.0192	retrograde calculation	1	[2]	-		-		-	
Unspecified	µL/min/mg	0.127	retrograde calculation	-		6.55	retrograde calculation	-		-	
CL_{renal}	L/h	0.157	retrograde calculation	3.6	[2]	1.2	[17]	-		1.5	[20]
Interactions											
CYP3A4 K_i	µM	-		-		10.5	[21]	40.3	[22]	42	[23]

CYP2C8 K_i	µM		-		-			4.8	[22]		-
CYP2C9 K_i	µM		-		-			19.5	[22]		-
CYP3A4 IndMax			-		16.68		[24]	9.5	[24]	8.34	optimized [b]
CYP3A4 IC_{50}	µM		-		0.32		[24]	3.9	[4]	0.3	[23]
CYP2B6 IndMax			-		-			5.7	[4]		-
CYP2B6 IC_{50}	µM		-		-			0.8	[4]		-
UGT1A1 IndMax			-		2.86		[17]	9.5	assumption [a]	1.43	optimized [b]
UGT1A1 IC_{50}	µM		-		0.32		[24]	3.9	assumption [a]	0.3	optimized [b]
UGT1A9 IndMax			-		5.48		[17]		-	2.74	optimized [b]
UGT1A9 IC_{50}	µM		-		0.32		[24]		-	0.3	optimized [b]

Abbreviations: BP, blood-plasma-ratio; Cl_{int}, intrinsic clearance; CL_{renal}, renal clearance; CYP, cytochrome P-450; fu_p, fraction unbound in plasma; IndMax, maximum fold of induction; IC_{50}, half maximal inhibitory concentration; K_m, Michaelis-Menten constant; K_i, inhibition constant; log P, octanol-water partition coefficient; ma, monoprotic acid; mb, monoprotic base; P_{app}, apparent permeability; pk_a, acid dissociation constant; UGT, uridine diphosphate-glucuronosyltransferase; V_{max}, maximum velocity.

[a] due to the scarcity of data for the strength of induction on UGT1A1 by efavirenz, it was assumed that IndMax and IC_{50} have the same value as CYP3A4 induction. This assumption was verified by running simulations for the concurrent administration of efavirenz and raltegravir (UGT1A1 substrate). Since the simulations were within 2-fold of observed clinical data, the assumption was considered valid.

[b] due to the scarcity of data for the strength of induction on CYP3A4, UGT1A1, and UGT1A9 by rifabutin, and since rifabutin is a moderate inducer, it was assumed that IndMax and IC_{50} were equal to half the value of IndMax and IC_{50} reported for rifampicin. This assumption was validated by running simulations with rilpivirine (CYP3A4 substrate), dolutegravir (CYP3A4, UGT1A1 substrate), raltegravir (UGT1A1 substrate), and cabotegravir (UGT1A1, UGT1A9 substrate). The simulations were within 2-fold of observed data; therefore, the assumption was considered valid.

Supplementary Table 2. Equations describing the age-related changes of a Caucasian healthy population.

Parameter	Unit	Descriptive equation	CV [%]
Body height	cm	$-0.0039 \times Age^2 + 0.238 \times Age - 12.5 \times Sex + 176$	3.8
Body weight	kg	$-0.0039 \times Age^2 + 1.12 \times Body\ height + 0.611 \times Age - 0.424 \times Sex - 137$	15.2
Lung weight	kg	$e^{(0.028 \times Body\ height + 0.0077 \times Age - 5.6)}$	0
Adipose weight	kg	$0.68 \times Body\ weight - 0.56 \times Body\ height + 6.1 \times Sex + 65$	29.6
Bone weight	kg	$e^{(0.024 \times Body\ height - 1.9)}$	13.2
Brain weight	kg	$e^{-0.0075 \times Age + 0.0078 \times Body\ height - 0.97}$	9.0
Gonad weight	kg	$-0.00034 \times Body\ weight - 0.00022 \times Age - 0.03 \times Sex + 0.072$	34.8
Heart weight	kg	$0.34 \times BSA + 0.0018 \times Age - 0.36$	17.9 (m), 22.7 (f)
Kidney weight	kg	$-0.00038 \times Age - 0.056 \times Sex + 0.33$	19.3 (m), 23.2 (f)
Muscle weight	kg	$17.9 \times BSA - 0.0667 \times Age - 5.68 \times Sex - 1.22$	11.8
Skin weight	kg	$e^{(-0.0058 \times Age - 0.37 \times Sex + 1.13)}$	8.3
Thymus weight	kg	0.0221	44.8
Gut weight	kg	$3E^{-06} \times Body\ height^{2.49}$	7.3
Spleen weight	kg	$e^{1.13 \times BSA - 3.93}$	51.7
Pancreas weight	kg	0.103	27.8
Liver weight	kg	$e^{(0.87 \times BSA - 0.0014 \times Age - 1.0)}$	23.7
Blood weight	kg	$e^{(0.067 \times BSA - 0.0025 \times Age - 0.38 \times Sex + 1.7)}$	10.4
Cardiac output (CO)	L/h	$159 \times BSA - 1.56 \times Age + 114$	21.1
Adipose blood flow	% of CO	$(0.044 + 0.027 \times Sex) \times Age + 2.4 \times Sex + 3.9$	
Bone blood flow	% of CO	5	
Brain blood flow	% of CO	$e^{-0.48 \times BSA + 0.04 \times Sex + 3.5}$	
Gonad blood flow	% of CO	$-0.03 \times Sex + 0.05$	
Heart blood flow	% of CO	$-0.72 \times Body\ height - 10 \times Sex + 134$	
Kidney blood flow	% of CO	$-8.7 \times BSA + 0.29 \times Body\ height - 0.081 \times Age - 13$	
Muscle blood flow	% of CO	$-6.4 \times Sex + 17.5$	
Skin blood flow	% of CO	5	
Thymus blood flow	% of CO	1.5	
Gut blood flow	% of CO	$2 \times Sex + 14$	
Parameter	Unit	Descriptive equation	CV [%]
Spleen blood flow	% of CO	3	

Pancreas blood flow	% of CO	1	
Liver blood flow	% of CO	$-0.108 \times Age + 1.04 \times Sex + 27.9$	
Albumin	g/L	$-0.0709 \times Age + 47.7$	7.9
GFR	mL/min	$e^{-0.0079 \times Age + 0.5 \times BSA + 4.2}$	14.7

Abbreviations: BSA, body surface area; CV, coefficient of variance; *f*, female; GFR, glomerular filtration rate; *m*, male.

Data reproduced from Stader et al. [25] with permission from the journal.

Supplementary Table 3. Observed vs predicted pharmacokinetic parameters for the DDI scenarios (steady-state condition).

	Absence perpetrator			In presence perpetrator			DDI ratio			Reference
	Observed	**Predicted**	**Ratio P/O**	**Observed**	**Predicted**	**Ratio P/O**	**Observed**	**Predicted**	**Ratio P/O**	
Dolutegravir (50 mg BID) – Rifampicin (600 mg)										
C_{max} [ng/mL]	5550 (49)	5184 (46)	0.93	3130 (25)	2272 (30)	0.73	0.56	0.44	0.78	
AUC_{0-T} [ng×h/mL]	46300 (55)	50601 (54)	1.09	21300 (31)	15754 (44)	0.74	0.46	0.31	0.68	[26]
C_{trough} [ng/mL]	2410 (77)	3165 (66)	1.31	670 (55)	514 (76)	0.77	0.28	0.16	0.58	
Dolutegravir (50 mg QD) – Efavirenz (600 mg)										
C_{max} [ng/mL]	3080 (30)	3376 (31)	1.10	1870 (42)	2470 (25)	1.32	0.61	0.73	1.21	
AUC_{0-T} [ng×h/mL]	42300 (39)	63748 (52)	1.51	18200 (50)	33571 (52)	1.84	0.43	0.53	1.22	[27]
C_{trough} [ng/mL]	910 (53)	1173 (69)	1.29	220 (76)	392 (88)	1.78	0.24	0.33	1.38	
Dolutegravir (50 mg QD) – Rifabutin (300 mg)										
C_{max} [ng/mL]	2950 (38)	3469 (30)	1.18	3410 (23)	2991 (25)	0.88	1.16	0.86	0.75	
AUC_{0-T} [ng×h/mL]	39100 (38)	52769 (43)	1.35	37000 (32)	41025 (38)	1.11	0.95	0.78	0.82	[26]
C_{trough} [ng/mL]	760 (43)	1121 (63)	1.48	530 (56)	719 (63)	1.36	0.70	0.64	0.92	
Raltegravir (400 mg BID) – Rifampicin (600 mg)										
C_{max} [ng/mL]	2966	2013 (25)	0.68	2929	1746 (21)	0.60	0.99	0.87	0.88	
AUC_{0-T} [ng×h/mL]	9910	7217 (33)	0.73	9278	6041 (22)	0.65	0.94	0.83	0.89	[28]
C_{trough} [ng/mL]	199	117 (66)	0.59	138	89 (41)	0.64	0.69	0.76	1.09	
Raltegravir (1200 mg single dose) – Efavirenz (600 mg)										
C_{max} [ng/mL]	6989 (134)	5864 (24)	0.84	6366 (133)	5237 (22)	0.82	0.91	0.89	0.98	
$AUC_{0-\infty}$ [ng×h/mL]	22303 (42)	22509 (40)	1.01	19186 (44)	18938 (29)	0.99	0.86	0.84	0.98	[29]
C_{trough} [ng/mL]	19 (50)	72 (95)	3.88 [+]	17 (48)	54 (69)	3.10 [+]	0.94	0.75	0.80	
Raltegravir (400 mg QD) – Rifabutin (300 mg)										
C_{max} [ng/mL]	2600 (92)	2199 (28)	0.85	3606 (92)	2129 (27)	0.59	1.39	0.97	0.70	
AUC_{0-T} [ng×h/mL]	8066 (75)	9002 (39)	1.12	9571 (184)	8526 (34)	0.89	1.19	0.95	0.80	[30]
C_{trough} [ng/mL] [*]	57 (55)	47 (78)	0.83	45 (52)	43 (69)	0.95	0.80	0.91	1.14	

Data are represented as geometric mean (CV). **Abbreviations:** AUC0-∞, area under the concentration-time curve to infinity; AUC_{0-T}, area under the concentration-time curve to the last time point; BID, administered twice a day; C_{max}, peak concentration; C_{trough}, trough concentration; DDI, drug-drug interaction; O, observed; P, predicted; QD, administered once a day.

* concentration measured at 12 hours

[+] The ratio observed:predicted of C_{trough} is outside 2-fold however the observed C_{trough} is very small also compared to the observed C_{max} making difficult to predict C_{trough} within 2-fold.

Supplementary Figure 1. Correlation between predicted vs observed (a) peak concentration (C_{max}), (b) area under the concentration-time curve (AUC), and (c) trough concentration (C_{trough}). The black line represents the identity line, the purple and the green lines represent the upper and lower limits, respectively proposed by Guest et al. [31], and the dashed black line represents the 2-fold range.

Abbreviations: AUC, area under the concentration-time curve; C_{max}, peak concentration; C_{trough}, trough concentration.

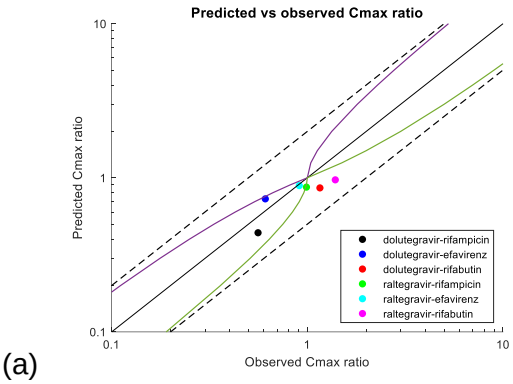

(a)

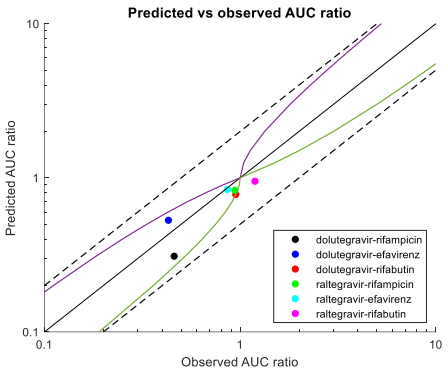

(b)

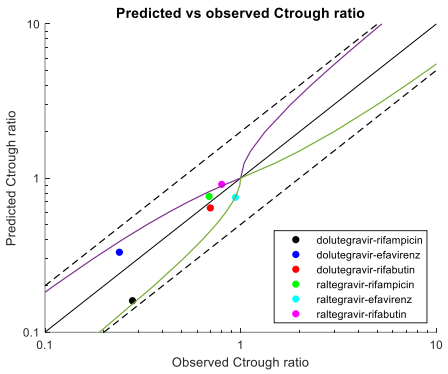

(c)

Supplementary Table 4. Observed vs predicted pharmacokinetic parameters during switch studies.

	Absence perpetrator			After stopping perpetrator			DDI ratio			Reference
	Observed	**Predicted**	**Ratio P/O**	**Observed**	**Predicted**	**Ratio P/O**	**Observed**	**Predicted**	**Ratio P/O**	
Rilpivirine 25 mg, oral administration - day 1 after stopping efavirenz										
C_{max} [ng/mL]	100 ± 28	129 ± 26	1.30	65 ± 21	71 ± 13	1.10	0.65	0.55	0.85	
AUC_{0-T} [ng×h/mL]	1095 ± 327	1236 ± 242	1.13	602 ± 204	648 ± 108	1.08	0.55	0.52	0.95	[32]
C_{trough} [ng/mL] *	33 ± 13 +	26 ± 8	0.78	13 ± 6 +	12 ± 3	0.92	0.40	0.47	1.18	
Rilpivirine 25 mg, oral administration - day 14 after stopping efavirenz										
C_{max} [ng/mL]	181 ± 45	181 ± 40	1.00	140 ± 34	173 ± 36	1.24	0.78	0.96	1.23	
AUC_{0-T} [ng×h/mL]	2528 ± 596	2413 ± 637	0.95	1940 ± 528	2246 ± 540	1.16	0.77	0.93	1.21	[32]
C_{trough} [ng/mL] *	67 ± 21	66 ± 22	0.98	47 ± 19	60 ± 18	1.27	0.70	0.91	1.29	
Rilpivirine 25 mg, oral administration e - day 21 after stopping efavirenz										
C_{max} [ng/mL]	181 ± 45	183 ± 41	1.01	154 ± 31	179 ± 38	1.16	0.85	0.98	1.15	
AUC_{0-T} [ng×h/mL]	2528 ± 596	2453 ± 664	0.97	2089 ± 526	2360 ± 597	1.13	0.83	0.96	1.16	[32]
C_{trough} [ng/mL] *	67 ± 21	68 ± 23	1.01	50 ± 21	64 ± 20	1.29	0.74	0.95	1.29	
Rilpivirine 25 mg, oral administration - day 28 after stopping efavirenz										
C_{max} [ng/mL]	181 ± 45	184 ± 41	1.01	166 ± 41	181 ± 40	1.10	0.92	0.99	1.08	
AUC_{0-T} [ng×h/mL]	2528 ± 596	2361 ± 638	0.93	2298 ± 548	2317 ± 600	1.01	0.91	0.98	1.08	[32]
C_{trough} [ng/mL] *	67 ± 21	68 ± 23	1.01	56 ± 23	66 ± 22	1.18	0.84	0.97	1.16	

Data represented as mean ± SD**. Abbreviations:** AUC_{0-T}, area under the concentration-time curve to the last time point; C_{max}, peak concentration; C_{trough}, trough concentration; DDI, drug-drug interaction; O, observed; P, predicted.

* Concentration measured 24h post-administration

+ digitalized data

Supplementary Figure 2. Correlation between predicted vs observed (a) switch scenario for peak concentration (C_{max}), (b) switch scenario for area under the concentration-time curve (AUC), and (c) switch scenario for trough concentration (C_{trough}). The black line represents the identity line, the purple and the green lines represent the upper and lower limits, respectively proposed by Guest et al. [31], and the dashed black line represents the 2-fold range.

Abbreviations: AUC, area under the concentration-time curve; C_{max}, peak concentration; C_{trough}, trough concentration.

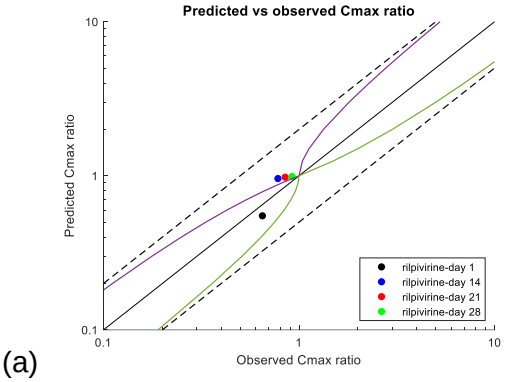

(a)

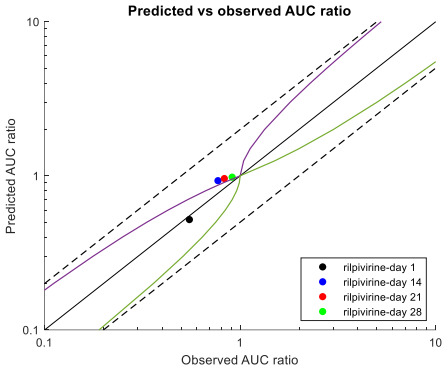

(b)

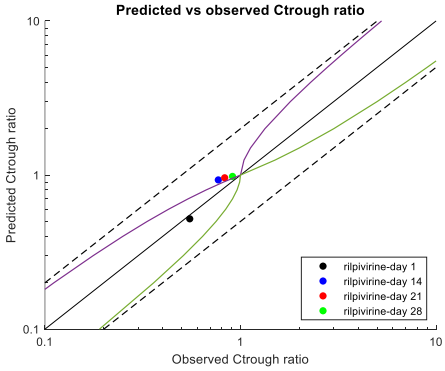

(c)

References

1. Rajoli RK, Back DJ, Rannard S, Freel Meyers CL, Flexner C, Owen A, et al. Physiologically based pharmacokinetic modelling to inform development of intramuscular long-acting nanoformulations for HIV. Clin Pharmacokinet. 2015 Jun;54(6):639-50.
2. Moss DM, Siccardi M, Back DJ, Owen A. Predicting intestinal absorption of raltegravir using a population-based ADME simulation. J Antimicrob Chemother. 2013 Jul;68(7):1627-34.
3. Varma MV, Lai Y, Feng B, Litchfield J, Goosen TC, Bergman A. Physiologically based modeling of pravastatin transporter-mediated hepatobiliary disposition and drug-drug interactions. Pharm Res. 2012 Oct;29(10):2860-73.
4. Molto J, Rajoli R, Back D, Valle M, Miranda C, Owen A, et al. Use of a physiologically based pharmacokinetic model to simulate drug-drug interactions between antineoplastic and antiretroviral drugs. J Antimicrob Chemother. 2017 Mar 1;72(3):805-11.
5. U.S. Food and Drug Administration. Mycobutin product label. 2021; Available from: https://www.accessdata.fda.gov/drugsatfda_docs/label/2014/050689Orig1s018lbl.pdf
6. Drugbanks. Dolutegravir. Available from: https://go.drugbank.com/drugs/DB08930
7. Stader F, Courlet P, Kinvig H, Battegay M, Decosterd LA, Penny MA, et al. Effect of ageing on antiretroviral drug pharmacokinetics using clinical data combined with modelling and simulation. Br J Clin Pharmacol. 2021 Feb;87(2):458-70.
8. Ke A, Barter Z, Rowland-Yeo K, Almond L. Towards a best practice approach in PBPK modeling: case example of developing a unified efavirenz model accounting for induction of CYPs 3A4 and 2B6. CPT Pharmacometrics Syst Pharmacol. 2016 Jul;5(7):367-76.
9. Vostrikov VV, Selishcheva AA, Sorokoumova GM, Shakina YN, Shvets VI, Savel'ev OY, et al. Distribution coefficient of rifabutin in liposome/water system as measured by different methods. Eur J Pharm Biopharm. 2008 Feb;68(2):400-5.
10. Blaschke TF, Skinner MH. The clinical pharmacokinetics of rifabutin. Clin Infect Dis. 1996 Apr;22 Suppl 1:S15-21; discussion S-2.
11. Gertz M, Harrison A, Houston JB, Galetin A. Prediction of human intestinal first-pass metabolism of 25 CYP3A substrates from in vitro clearance and permeability data. Drug Metab Dispos. 2010 Jul;38(7):1147-58.
12. Skinner MH, Blaschke TF. Clinical pharmacokinetics of rifabutin. Clin Pharmacokinet. 1995 Feb;28(2):115-25.
13. Kobayashi M, Yoshinaga T, Seki T, Wakasa-Morimoto C, Brown KW, Ferris R, et al. In Vitro antiretroviral properties of S/GSK1349572, a next-generation HIV integrase inhibitor. Antimicrob Agents Chemother. 2011 Feb;55(2):813-21.
14. Gele T, Gouget H, Furlan V, Becker PH, Taburet AM, Lambotte O, et al. Characteristics of dolutegravir and bictegravir plasma protein binding: a first approach for the study of pharmacologic sanctuaries. Antimicrob Agents Chemother. 2020 Oct 20;64(11).
15. Barau C, Furlan V, Yazdanpanah Y, Fagard C, Molina JM, Taburet AM, et al. Characterization of binding of raltegravir to plasma proteins. Antimicrob Agents Chemother. 2013 Oct;57(10):5147-50.
16. Boman G, Ringberger VA. Binding of rifampicin by human plasma proteins. Eur J Clin Pharmacol. 1974 Aug 23;7(5):369-73.
17. Gufford BT, Robarge JD, Eadon MT, Gao H, Lin H, Liu Y, et al. Rifampin modulation of xeno- and endobiotic conjugating enzyme mRNA expression and associated microRNAs in human hepatocytes. Pharmacol Res Perspect. 2018 Apr;6(2):e00386.
18. Wanke R, Harjivan SG, Pereira SA, Marques MM, Antunes AM. The role of competitive binding to human serum albumin on efavirenz-warfarin interaction: a nuclear magnetic resonance study. Int J Antimicrob Agents. 2013 Nov;42(5):443-6.
19. Pfizer Canada ULC. Product Monograph Mycobutin (rifabutin capsule USP). 2003; Available from: https://www.pfizer.ca/sites/default/files/202102/MYCOBUTIN_PM_E_244143_11Feb2021.pdf

20. Skinner MH, Hsieh M, Torseth J, Pauloin D, Bhatia G, Harkonen S, et al. Pharmacokinetics of rifabutin. Antimicrob Agents Chemother. 1989 Aug;33(8):1237-41.
21. Sun Y, Chothe PP, Sager JE, Tsao H, Moore A, Laitinen L, et al. Quantitative prediction of CYP3A4 induction: impact of measured, free, and intracellular perpetrator concentrations from human hepatocyte induction studies on drug-drug interaction predictions. Drug Metab Dispos. 2017 Jun;45(6):692-705.
22. Marzolini C, Rajoli R, Battegay M, Elzi L, Back D, Siccardi M. Physiologically based pharmacokinetic modeling to predict drug-drug interactions with efavirenz involving simultaneous inducing and inhibitory effects on cytochromes. Clin Pharmacokinet. 2017 Apr;56(4):409-20.
23. McGinnity DF, Zhang G, Kenny JR, Hamilton GA, Otmani S, Stams KR, et al. Evaluation of multiple in vitro systems for assessment of CYP3A4 induction in drug discovery: human hepatocytes, pregnane X receptor reporter gene, and Fa2N-4 and HepaRG cells. Drug Metab Dispos. 2009 Jun;37(6):1259-68.
24. Almond LM, Mukadam S, Gardner I, Okialda K, Wong S, Hatley O, et al. Prediction of Drug-drug interactions arising from CYP3A induction using a physiologically based dynamic model. Drug Metab Dispos. 2016 Jun;44(6):821-32.
25. Stader F, Siccardi M, Battegay M, Kinvig H, Penny MA, Marzolini C. Repository describing an aging population to inform physiologically based pharmacokinetic models considering anatomical, physiological, and biological age-dependent changes. Clin Pharmacokinet. 2019 Apr;58(4):483-501.
26. Dooley KE, Sayre P, Borland J, Purdy E, Chen S, Song I, et al. Safety, tolerability, and pharmacokinetics of the HIV integrase inhibitor dolutegravir given twice daily with rifampin or once daily with rifabutin: results of a phase 1 study among healthy subjects. J Acquir Immune Defic Syndr. 2013 Jan 1;62(1):21-7.
27. Song I, Borland J, Chen S, Guta P, Lou Y, Wilfret D, et al. Effects of enzyme inducers efavirenz and tipranavir/ritonavir on the pharmacokinetics of the HIV integrase inhibitor dolutegravir. Eur J Clin Pharmacol. 2014 Oct;70(10):1173-9.
28. Taburet AM, Sauvageon H, Grinsztejn B, Assuied A, Veloso V, Pilotto JH, et al. Pharmacokinetics of raltegravir in HIV-infected patients on rifampicin-based antitubercular therapy. Clin Infect Dis. 2015 Oct 15;61(8):1328-35.
29. Krishna R, East L, Larson P, Siringhaus T, Herpok L, Bethel-Brown C, et al. Efavirenz does not meaningfully affect the single dose pharmacokinetics of 1200 mg raltegravir. Biopharm Drug Dispos. 2016 Dec;37(9):542-9.
30. Brainard DM, Kassahun K, Wenning LA, Petry AS, Liu C, Lunceford J, et al. Lack of a clinically meaningful pharmacokinetic effect of rifabutin on raltegravir: in vitro/in vivo correlation. J Clin Pharmacol. 2011 Jun;51(6):943-50.
31. Guest EJ, Aarons L, Houston JB, Rostami-Hodjegan A, Galetin A. Critique of the two-fold measure of prediction success for ratios: application for the assessment of drug-drug interactions. Drug Metab Dispos. 2011 Feb;39(2):170-3.
32. Crauwels H, Vingerhoets J, Ryan R, Witek J, Anderson D. Pharmacokinetic parameters of once-daily rilpivirine following administration of efavirenz in healthy subjects. Antivir Ther. 2012;17(3):439-46.